Steering magnetization dynamics of nanoparticles with ultrashort pulses

A. Sukhov[1,2] and J. Berakdar[2]
[1]*Max-Planck-Institut für Mikrostrukturphysik, Weinberg 2, D-06120 Halle/Saale, Germany*
[2]*Institut für Physik, Martin-Luther-Universität Halle-Wittenberg, Heinrich-Damerow-Str. 4, 06120 Halle, Germany*
(Received 21 January 2009; revised manuscript received 2 April 2009; published 28 April 2009)

A scheme is proposed for steering the magnetization of a monodomain nanoparticle to a predefined state via ultrashort magnetic pulses. Based on the Landau-Lifshitz-Gilbert equation we find analytical expressions for the driving fields and the magnetization dynamics valid for pulse durations shorter than the field-free precessional period of the magnetization. These expressions do not depend on the type of anisotropy and provide conditions for fast switching and magnetization "freezing." Numerically, using the Landau-Lifshitz-Gilbert equation extended to finite temperatures we confirm the robustness of the analytical predictions to thermal fluctuations, different anisotropy types, and shapes of pulses; and also explore the range of validity of the short-pulse approximation.

DOI: 10.1103/PhysRevB.79.134433 PACS number(s): 75.10.Hk, 75.40.Gb, 75.40.Mg

I. INTRODUCTION

Ongoing experimental and theoretical researches on nanomagnetism are fueled by various technological applications such as high-density storage media and fast sensors.[1–3] The efficient operation of storage devices with a high density entails a high-rate recording method, i.e., a procedure for fast magnetization switching. To meet this demand several techniques for magnetization reversal were explored: Making use of the inverse Faraday effect the spin dynamics can be triggered by a laser.[4–6] Extensive experimental and theoretical researches were also devoted to the reversal process by means of external static or alternating magnetic fields.[7–16] A currently active area of research is the magnetization dynamics driven either by a spin torque or pulses of spin torques[17] that are generated by appropriate spin polarized electric current.[18–25] As shown by several studies,[26–34] transverse magnetic fields and field pulses are further efficient means for fast switching and may allow, upon duration control,[2,32] for a quasiballistic magnetization switching.

Here we address the issue of the magnetization switching of monodomain magnetic nanoparticles from the perspective of control strategies; in particular we make use of the ideas of the local-control theory (LCT).[35–37] LCT is applied mostly in quantum chemistry where a number of other control methods[35,36,38,39] are used. The basic idea of LCT is to derive the control fields; in our case the parameters of the magnetic field pulses, from the response of the system, i.e., from the magnetization evolution.[34] Obviously, such a scheme leads to an iterative procedure where a field pulse starts the magnetization evolution whose details determine the next field pulses that allow for a magnetization steering. In the event that the pulse durations are small on the scale of the magnetization precessional period we are able to derive transparent analytical expressions for this LCT scheme for determining the type of pulses that lead to a fast controlled switching or stabilizing the magnetization around a predefined state, an effect which we call magnetization "freezing." The scenario for the magnetization dynamics that emerges from our scheme is that sudden impulsive magnetic field kicks guide the magnetization toward the desired direction. In between the pulses field-free precessions and relaxation take place. The efficiency and the robustness of the scheme to thermal fluctuations are tested by performing finite-temperature full numerical calculations and considering different types of anisotropy.

II. ANALYTICAL MODEL

We consider FePt and cobalt nanoparticles that have a uniaxial anisotropy [$Fe_{50}Pt_{50}$ (Refs. 3 and 40); Co (Ref. 41)] and a cubic anisotropy [$Fe_{70}Pt_{30}$ (Refs. 3 and 42)]. The particle magnetic dynamics can be modeled by the classical evolution of a large classical magnetic moment (Stoner nanoparticle[2]). The classical dynamics of such a magnetic moment is governed by the Landau-Lifshitz-Gilbert (LLG) equations.[43,44] The precessional motion of the magnetization is described by the time evolution of the two independent angles ϕ (azimuthal angle) and θ (polar angle). When including the (constant) Gilbert damping α,[44] the LLG reads as[2]

$$(1+\alpha^2)\frac{d\phi}{dt} = \frac{1}{\sin\theta}\cdot\frac{\partial\mathcal{H}}{\partial\theta} - \frac{\alpha}{\sin^2\theta}\cdot\frac{\partial\mathcal{H}}{\partial\phi},$$

$$(1+\alpha^2)\frac{d\theta}{dt} = -\frac{1}{\sin\theta}\cdot\frac{\partial\mathcal{H}}{\partial\phi} - \alpha\cdot\frac{\partial\mathcal{H}}{\partial\theta}, \tag{1}$$

where the total energy is given by

$$\mathcal{H} = \mathcal{H}_A + \mathcal{H}_F = \mathcal{H}_A - \mathbf{S}\cdot\mathbf{b}_0(t). \tag{2}$$

The energy is measured in units of $\mu_S B_A$. Here μ_S denotes the magnetic moment of the nanoparticle at saturation, $B_A = 2D/\mu_S$ is the anisotropy field and D is the anisotropy energy density. $\mathcal{H}_A$ and $\mathcal{H}_F$ are, respectively, the contributions from the anisotropy and the interaction with the external magnetic field $\mathbf{b}_0(t)$. Time is expressed in the units of the

field-free precessional time $T^{\text{prec}}=2\pi/[\gamma(2D/\mu_S)]$ (which is ~ 5 ps for a 6 nm large $Fe_{50}Pt_{50}$ nanoparticle[45]), where γ is a gyromagnetic ratio. For the control scheme we consider magnetic pulses of the form

$$\mathbf{b}_0(t)=\begin{cases}\dfrac{f(t)b_0}{2\varepsilon}(\cos\phi_0\mathbf{e}_x+\sin\phi_0\mathbf{e}_y), & t_0-\epsilon<t<t_0+\epsilon\\ 0, & \text{elsewhere.}\end{cases}, \tag{3}$$

$\mathbf{e}_{x/y}$ are units vectors along the x and y axes. Equation (3) is realizable by two perpendicular magnetic fields $\mathbf{b}_x$ and $\mathbf{b}_y$ each having a duration 2ε and a shape (envelope function) $f(t)$ centered at some time moment $t=t_0$. Their relative strength is characterized by the mock angle ϕ_0, with $\tan\phi_0=|b_y|/|b_x|$. The exerted total field strength is $|f|b_0/(2\varepsilon)$, i.e., $\mathbf{b}_0(t)=\mathbf{b}_x+\mathbf{b}_y$. To achieve shorter switching times and/or lower switching fields we may optimize the geometries of the applied fields. This point has been proposed in a recent work[46] for static magnetic fields. For the type of fields employed in this work, this is also true as confirmed by some test calculations that we performed.

For the total energy change one finds

$$\frac{\partial\mathcal{H}}{\partial\phi}=\frac{\partial\mathcal{H}_A}{\partial\phi}+\frac{\partial\mathcal{H}_F}{\partial\phi}=\frac{\partial\mathcal{H}_A}{\partial\phi}+\frac{b_0f(t)}{2\varepsilon}\sin\theta\sin(\phi-\phi_0),$$

$$\frac{\partial\mathcal{H}}{\partial\theta}=\frac{\partial\mathcal{H}_A}{\partial\theta}+\frac{\partial\mathcal{H}_F}{\partial\theta}=\frac{\partial\mathcal{H}_A}{\partial\theta}-\frac{b_0f(t)}{2\varepsilon}\cos\theta\cos(\phi-\phi_0).$$

The new dimensionless variable $\tau(t)$,

$$\tau(t)=\frac{t-(t_0+\varepsilon)+2\varepsilon}{2\varepsilon},\quad \frac{d\tau}{dt}=\frac{1}{2\varepsilon}, \tag{4}$$

has the property

$$\tau=0\ \text{ for }\ t=t_0-\varepsilon,$$

$$\tau=1\ \text{ for }\ t=t_0+\varepsilon. \tag{5}$$

In τ the system evolves according to

$$\frac{1}{2\varepsilon}\frac{d\phi}{d\tau}=p\left[\frac{1}{\sin\theta}\frac{\partial\mathcal{H}_A}{\partial\theta}-\frac{\alpha}{\sin^2\theta}\frac{\partial\mathcal{H}_A}{\partial\phi}\right]-\frac{pb_0f[t(\tau)]}{2\varepsilon}\left[\frac{\cos\theta}{\sin\theta}\cos\delta\phi+\alpha\frac{\sin\delta\phi}{\sin\theta}\right],$$

$$\frac{1}{2\varepsilon}\frac{d\theta}{d\tau}=p\left[-\frac{1}{\sin\theta}\frac{\partial\mathcal{H}_A}{\partial\phi}-\alpha\frac{\partial\mathcal{H}_A}{\partial\theta}\right]+\frac{pb_0f[t(\tau)]}{2\varepsilon}[-\sin\delta\phi+\alpha\cos\theta\cos\delta\phi], \tag{6}$$

where we introduced the notation

$$\delta\phi=\phi-\phi_0,\quad p=\frac{1}{1+\alpha^2}.$$

We recall that the time scale in Eqs. (4) and (6) is set by the precessional period T^{prec} which itself is set by the anisotropy energy. From Eq. (6) it follows that when $\varepsilon\to 0$ (valid for $\varepsilon\ll T^{\text{prec}}$), the effect of anisotropy is negligible during and right after the pulse. Thus, on time scales $|t-t_0|\ll 1$ the magnetic dynamics is governed only by the parameters $\delta\phi$, α, and b_0 regardless of the type of anisotropy. In Sec. III the dynamics of the magnetization will be considered separately during and right after the pulse application (excitation) and for the field-free motion (precession and relaxation).

III. ANALYTICAL TREATMENT

A. Field-free nanoparticle with a uniaxial anisotropy

In the absence of a magnetic pulse, i.e., for $b_0=0$ in Eq. (6), and for a uniaxial anisotropy described by

$$\mathcal{H}_A^U=-\frac{1}{2}\cos^2\theta, \tag{7}$$

the solution of the LLG equations is well known [cf., e.g., Ref. 47 (Eqs. (A4) and (A10)]. For the initial conditions angles $\phi_f(t=\bar{t}_0)$ and $\theta_f(t=\bar{t}_0)$ one finds

$$\phi_f(t)=\phi(\bar{t}_0)\pm\frac{t-\bar{t}_0}{1+\alpha^2}\pm\frac{1}{\alpha}\ln\left|\frac{\cos\theta_f(\bar{t}_0)(1+\sqrt{1+\tan^2\theta_f(\bar{t}_0)\cdot e^{-2\alpha(t-\bar{t}_0)/1+\alpha^2}})}{1+\cos\theta_f(\bar{t}_0)}\right|,$$

$$\tan\theta_f(t)=\tan\theta_f(\bar{t}_0)\cdot e^{-\alpha/1+\alpha^2(t-\bar{t}_0)}. \tag{8}$$

"+" or "−" refer to $0<\theta<\pi/2$ or $\pi/2<\theta<\pi$, respectively. This solution indicates that the system relaxes through precessions to one of two energy minima, i.e., $\theta_{f,\min 1}=0$ or $\theta_{f,\min 2}=\pi$.

B. Field-free nanoparticle with a cubic anisotropy

In the absence of magnetic pulses for a system with a cubic anisotropy,[48] i.e., when

$$\mathcal{H}_A^C = -\frac{1}{2}(\cos^2\phi \sin^2\phi \sin^4\theta + \cos^2\theta \sin^2\theta), \quad (9)$$

the equations governing the magnetization dynamics are

$$\frac{d\phi}{dt} = -\frac{1}{1+\alpha^2}\cos\theta\left(\frac{1}{2}\sin^2 2\phi \sin^2\theta + \cos 2\theta\right) + \frac{1}{4}\frac{\alpha}{1+\alpha^2}\sin^2\theta \sin 4\phi,$$

$$\frac{d\theta}{dt} = +\frac{1}{4}\frac{1}{1+\alpha^2}\sin^3\theta \sin 4\phi + \frac{1}{2}\frac{\alpha}{1+\alpha^2}\sin 2\theta\left(\frac{1}{2}\sin^2 2\phi \sin^2\theta + \cos 2\theta\right). \quad (10)$$

The solution of these equations has to be performed numerically. We note, however, that if ϕ varies slowly (e.g., as in thin films), Eq. (10) admits an approximate analytical solution. The analytical methods outlined below rely on a short-time evolution for which the type of anisotropy during the action of the external driving is not important (as discussed above).

C. Nanoparticle subject to ultrashort magnetic pulses

Applying the ultrashort magnetic pulses $\mathbf{b}_0(t)$, i.e., pulses with durations $\varepsilon \ll T^{\text{prec}}$, we obtain from Eq. (6)

$$\frac{d\phi}{d\tau} = -\frac{1}{\sin\theta}\frac{b_0 f[t(\tau)]}{1+\alpha^2}[\cos\theta\cos\delta\phi + \alpha\sin\delta\phi],$$

$$\frac{d\theta}{d\tau} = \frac{b_0 f[t(\tau)]}{1+\alpha^2}[-\sin\delta\phi + \alpha\cos\theta\cos\delta\phi]. \quad (11)$$

These equations describe a stroboscopic evolution; i.e., they determine $\theta(t^+)$ and $\phi(t^+)$ right after the pulses for some defined conditions before the pulses $\theta(t^-)$ and $\phi(t^-)$. No information is provided on the evolution during the pulse. Here we use the notation $t^- := t_0 - \varepsilon$ and $t^+ = t_0 + \varepsilon$. In the local-control theory[37–39] the control field that drives the system to achieve a desired property is derived from the response of the system. In the context of switching we define the control condition as

$$\theta(t^+) > \theta(t^-) \quad \forall\, t^+, t^-, \quad (12)$$

meaning that the polar angle has to increase upon the pulse application (no condition is set on ϕ). An analytical expression for the controlled evolution in line with Eq. (12) is obtainable, for instance, for $\delta\phi = 0$ or $\delta\phi = 3\pi/2$.

1. Solution for $\delta\phi = 0$

We apply a sequence of the pulses [Eq. (3)] $i = 1 \ldots N$ with the same durations and each pulse is centered at the time moment $t_{0,i}$. For $\delta\phi = 0$, i.e., when for a pulse the field strength ratio $\phi_{i,0}$ is equal the temporal (at $t_{i,0}$) magnetization azimuthal angle ϕ, we find for the solution of Eq. (11) the following changes in θ and ϕ right after the ith pulse,

$$\phi(t_i^+) = \phi(t_i^-) - \ln\left|\tan\left(\frac{\theta(t_i^+)}{2}\right)\cdot\frac{\tan\left(\frac{\theta(t_i^-)}{2}+\frac{\pi}{4}\right)+1}{\tan\left(\frac{\theta(t_i^-)}{2}+\frac{\pi}{4}\right)-1}\right|,$$

$$\tan\left(\frac{\theta(t_i^+)}{2}\right) = \frac{\tan\left(\frac{\theta(t_i^-)}{2}+\frac{\pi}{4}\right)\cdot e^{\alpha b_0 f(t_{0,i})/1+\alpha^2} - 1}{\tan\left(\frac{\theta(t_i^-)}{2}+\frac{\pi}{4}\right)\cdot e^{\alpha b_0 f(t_{0,i})/1+\alpha^2} + 1}. \quad (13)$$

We remark that the pulse-induced change in θ is not uniform. It depends on the prior-pulse angle $\theta(t_i^-)$ and increases as a complicated function of it. As for the dependence on damping, for $\alpha \to 0$ switching becomes ineffective since there are no changes in θ (the second equation of system (13) gives $\tan[\theta(t_i^+)/2] = \tan(\theta(t_i^-)/2)$) and in ϕ $[\phi(t_i^+) = \phi(t_i^-)]$. For sufficiently high damping $(\alpha > 1)$ $\theta(t_i^+) \to \pi/2$ and $\phi(t_i^+)$ strongly depends on $\theta(t_i^-)$. Concerning $d\theta/d\tau > 0$ we conclude from Eq. (11) that the sign of $d\theta/d\tau$ depends on $\cos\theta$, i.e., whether $0 < \theta < \pi/2$ or $\pi/2 < \theta < \pi$, meaning that one chooses $\delta\phi = 0$ for $0 < \theta < \pi/2$ and $\delta\phi = \pi$ for $\pi/2 < \theta < \pi$ to obtain the complete magnetization reversal.

2. Solution for $\delta\phi = 3\pi/2$

For the control condition $\delta\phi = 3\pi/2$ we derive

$$\phi(t_i^+) = \phi(t_i^-) + \alpha \ln\left|\frac{\tan\left(\frac{\theta(t_i^-)}{2} + \frac{1}{2}\frac{b_0 f(t_{0,i})}{1+\alpha^2}\right)}{\tan\left(\frac{\theta(t_i^-)}{2}\right)}\right|,$$

$$\theta(t_i^+) = \theta(t_i^-) + \frac{b_0 f(t_{0,i})}{1+\alpha^2}. \quad (14)$$

We observe a uniform pulse-induced increase in θ with an amount that depends on the field amplitude b_0. Another important feature is that for small dissipation this increase only slightly depends on damping and is proportional to the applied field leading thus to rapid changes in the z projection of the magnetization. Additionally, in the low damping regime ϕ remains almost unchanged which makes this regime very effective for switching (ballistic switching). Only small changes in θ and ϕ occur if the damping becomes large.

3. Solution for general $\delta\phi$

The second equation of Eq. (11) can be solved for $\delta\phi$ in a general form. For $\theta(t_i^-)$ and $\theta(t_i^+)$ the solution reads

$$\left|2\sqrt{2}\,\text{arctanh}\left[\frac{\sqrt{1+\cos 2\delta\phi}}{\cos\delta\phi}\frac{(\alpha\cos\delta\phi + \sin\delta\phi)\tan\frac{\theta}{2}}{\sqrt{\alpha^2 - 1 + (\alpha^2+1)\cos 2\delta\phi}}\right]\right|_{\theta(t_i^-)}^{\theta(t_i^+)} = \frac{b_0 f(t_{0,i})}{1+\alpha^2}\cdot\sqrt{\alpha^2 - 1 + (\alpha^2+1)\cos 2\delta\phi}. \quad (15)$$

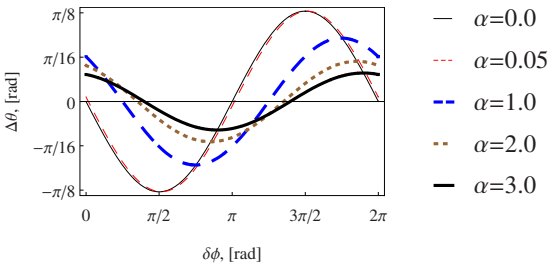

FIG. 1. (Color online) Change in angle θ directly after the ith pulse as a function of $\delta\phi$ plotted for different values of damping α. Other parameters: $b_0=0.4$, $\theta(t_i^-)=\pi/180$, and $f(t_{0,i})=1$.

The quantity of interest is $\Delta\theta_i=\theta(t_i^+)-\theta(t_i^-)$ as a function of $\delta\phi$. The knowledge of $\Delta\theta_i(\delta\phi)$ is of a particular importance when it comes to the question of the role of thermal fluctuations. The issue here is to identify the conditions/parameters for which we achieve a maximal positive tilt angle upon the pulse. The results in Figs. 1 and 2 show the dependence of $\Delta\theta_i(\delta\phi)$ [graphical illustration of Eq. (15)].

Figure 1 indicates a positive tilt angle in the range around $\pi<\phi_+<2\pi$. The black thin curve for $\alpha=0$ shows no increase in $\Delta\theta_i$ for $\delta\phi=0$ [consistent with the second equation of Eq. (11)] since only precession is possible. For $3\pi/2$ the maximum of $\Delta\theta_i$ is achievable even for $\alpha=0$. This finding is consistent with the second equation of Eq. (14), where the change in θ upon the pulse is positive and proportional to the field amplitude b_0 for small α. The reason for this effect is that the applied field is then tuned to exert a large moment on the magnetization. Other trends deducible from this figure are: a further increase in damping leads only to smaller $\Delta\theta_i$ whereas the maxima of the peaks shift toward smaller $\delta\phi$. Note that a change in the period of $\delta\phi$ is not accessible. It always remains the same 2π, meaning that there are two regimes: If $0<\delta\phi<\pi$ the change is negative, whereas for $\pi<\delta\phi<2\pi$ this quantity is positive. Figure 2 depicts $\Delta\theta_i(\delta\phi)$ dependence for various field amplitudes. A general trend here is that for higher field amplitudes larger angular changes are achievable. For high amplitudes (from $b_0=2.0$) switching is possible with only one pulse since $\Delta\theta_i>\pi/2$. The period of $\delta\phi$ remains the same as for Fig. 1, namely, 2π.

Concerning the case of finite temperatures $T\neq 0$ K, the magnetization direction, in particular ϕ, should be assumed to be shifted randomly with respect to ϕ_0. For this reason, an analytical expression for $\Delta\theta_i(\delta\phi)$ is not available. However,

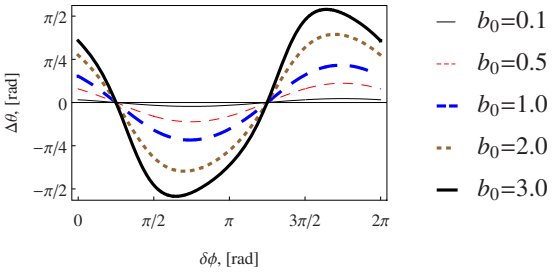

FIG. 2. (Color online) Change in θ right after the ith pulse as a function of $\delta\phi$ shown for different field amplitudes b_0. Further parameters: $\alpha=1.0$, $\theta(t_i^-)=\pi/180$, and $f(t_{0,i})=1$.

from the preceding discussion we can conclude that the most optimal conditions for switching are when $\delta\phi=3\pi/2$ or close to it and for small damping. Both conditions can be fulfilled highly precisely, allowing thus for a finite-temperature control of the magnetization.

4. Solution for general $\delta\phi$ and $\alpha\to 0$

Assuming $\alpha\to 0$ in Eq. (11) we find the following solution:

$$\phi(t_i^+)=\phi(t_i^-)-\frac{\cos\,\delta\phi}{\sin\,\delta\phi}\ln\left|\frac{\tan[\theta(t_i^-)-b_0 f(t_{0,i})\sin\,\delta\phi]}{\sin\,\theta(t_i^-)}\right|,$$

$$\theta(t_i^+)=\theta(t_i^-)-b_0 f(t_{0,i})\sin\,\delta\phi. \tag{16}$$

Similar to Eq. (14) we conclude that switching is mostly effective if $\delta\phi=3\pi/2$ which leads to a uniform change in θ and hardly any changes in ϕ. Pulses applied in this way would lead only to a precessional motion of the magnetization. The relation for θ, as given by Eq. (16), is consistent with the results presented in Fig. 1 for $\alpha=0$ (the thin black curve).

5. Critical field amplitudes needed for reversal for a sequence of pulses with fixed $\delta\phi$

Above we discussed the influence of $\delta\phi$ on the magnetization reversal control. Another relevant parameter is the field amplitude. Here we attempt to find the minimum field amplitudes needed for pulse-assisted reversal. We note that the idea of deriving the critical fields has already been developed, e.g., in Ref. 49, however without the short-pulse approximation. For a magnetization reversal, an obvious requirement on the external field would be that the change in θ induced by the ith pulse, i.e., $\Delta\theta_i^{\text{excit}}=\theta(t_i^+)-\theta(t_i^-)$, should be not less than the subsequent (until the next pulse $i+1$) relaxation, $\Delta\theta_i^{\text{relax}}=\theta(t_{i+1}^-)-\theta(t_i^+)$ or

$$\Delta\theta_i^{\text{excit}}\geq|\Delta\theta_i^{\text{relax}}|. \tag{17}$$

A critical field amplitudes is achieved when $\Delta\theta_i^{\text{excit}}=\Delta\theta_i^{\text{relax}}$.

From Eq. (8) we find that

$$\Delta\theta_i^{\text{relax}}=\arctan\{\tan[\theta(t_i^-)]\cdot e^{\alpha\tau_i/1+\alpha^2}\}-\theta(t_i^-), \tag{18}$$

where τ_i is the time lag during relaxation.

Inspecting Eqs. (18) and (14) we deduce the critical field value needed to switch the magnetization using magnetic pulses ($\delta\phi_i=3\pi/2$ for all pulses),

$$b_{0\text{cr}}^{(\delta\phi_i=3\pi/2)}=(1+\alpha^2)\{\arctan[\tan(\theta(t_i^-))\cdot e^{\alpha\tau_i/1+\alpha^2}]-\theta(t_i^-)\}. \tag{19}$$

Similarly for $\delta\phi_i=0$ we use Eqs. (18) and (13) and obtain for the critical field

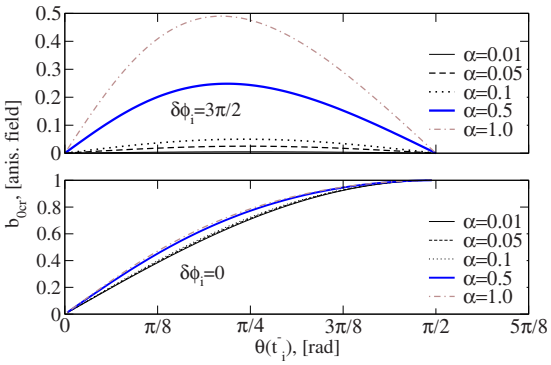

FIG. 3. (Color online) Dependence of the critical field amplitude $b_{0\mathrm{cr}}$ on the angle $\theta(t_i^-)$ at the beginning of pulse application for $\delta\phi_i=3\pi/2$ and $\delta\phi_i=0$. Pulses are applied with a delay of the precessional period.

$$b_{0\mathrm{cr}}^{(\delta\phi_i=0)} = -\frac{1+\alpha^2}{\alpha}\ln\left\{\tan\left[\frac{\theta(t_i^-)}{2}+\frac{\pi}{4}\right]\right\} + \frac{1+\alpha^2}{\alpha}\ln\left\{\frac{1+\tan\left[\frac{1}{2}\arctan(\tan(\theta(t_i^-))\cdot e^{\alpha\tau_i/1+\alpha^2}\right]}{1-\tan\left[\frac{1}{2}\arctan(\tan(\theta(t_i^-))\cdot e^{\alpha\tau_i/1+\alpha^2}\right]}\right\}. \quad (20)$$

Dependencies (19) and (20) are shown in Fig. 3 for $\tau_i = T^{\mathrm{Prec}}$. From these results we conclude: to switch the magnetization a lower critical field can be applied if $\theta(t_i^-)$ is (roughly) known. Otherwise one can apply the (possibly larger) critical field deduced from the maximum of the graph shown in Fig. 3. The above analytical expressions are achieved for the condition that the delay time τ_i is constant for all pulses. The question of whether $b_{0\mathrm{cr}}[\theta(t_i^-)]$ changes if τ_i is not constant is addressed in Fig. 4. For $\delta\phi_i=3\pi/2$ an exponentially increasing repetition of pulses gives rise to an increase in critical field amplitudes. Further changes in τ_i dependence for $\delta\phi_i=3\pi/2$ have a minor effect on the $b_{0\mathrm{cr}}[\theta(t_i^-)]$ dependence. In the case of $\delta\phi_i=0$ various τ_i dependencies modify strongly $b_{0\mathrm{cr}}[\theta(t_i^-)]$.

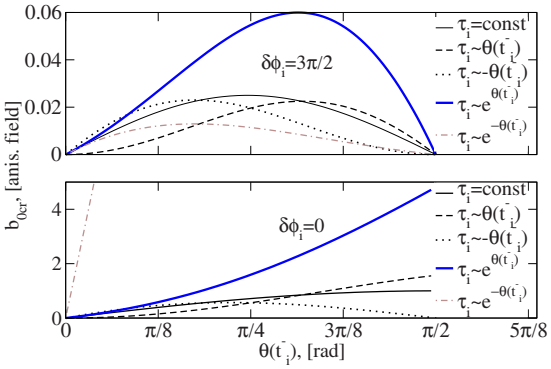

FIG. 4. (Color online) Critical-field-amplitude dependence on $\theta(t_i^-)$ right before the pulse for $\delta\phi_i=3\pi/2$ and $\delta\phi_i=0$ for $\alpha=0.05$. Pulses are applied with various delay times.

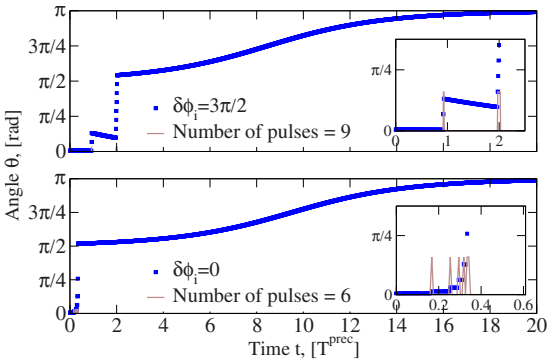

FIG. 5. (Color online) Evolution of $\theta(t)$ for $\delta\phi_i=3\pi/2$ and $\delta\phi_i=0$. Other parameters: $\phi_f(0)=\pi/180$, $\theta_f(0)=\pi/180$, $\phi_0=\pi/3$, $\alpha=0.05$, $b_0=0.2$, and $f(t_{0,i})=1$. Insets show the detailed motion at the beginning of the pulse application (field amplitudes enlarged $\times 5$).

6. Sequence of magnetic pulses for fixed $\delta\phi$

For certain field strength ratio ϕ_0 we allow at first for a field-free propagation [starting from some initial $\phi_f(0)$ and $\theta_f(0)$] until $\phi_f(t)$ is such that $\delta\phi$ is 0 or $3\pi/2$. At this moment the pulses are applied and the angular change in θ and ϕ is calculated according to formula (13) or (14), respectively. Figure 5 illustrates this procedure and the process of the reversal in the small damping regime which is appropriate for magnetic nanoparticles. There are certain differences when choosing $\delta\phi_i=3\pi/2$ or $\delta\phi_i=0$: for $\delta\phi_i=3\pi/2$ the increase in θ comes about due to equidistant jumps [Eq. (14)], whereas for $\delta\phi_i=0$ the length of jumps depends on the current ϕ,θ coordinate. In the vicinity of $\theta=\pi/2$ the jumps are higher. For this reason the switching is faster for $\delta\phi_i=0$ than for $\delta\phi_i=3\pi/2$ with a total number of pulses 6 and 9, respectively. The total switching field is $6\times0.2=1.2$ and $9\times0.2=1.8$, respectively. Thus, based on Fig. 5 we argue that the efficient way to switch the magnetization is to apply a pulse at $\delta\phi_i=3\pi/2$ for $0<\theta<\pi/4$ and at $\delta\phi_i=0$ for $\pi/4<\theta<\pi/2$. The reason why the switching is possible for $\delta\phi_i=3\pi/2$ with field amplitude $b_0=0.2$ directly follows from Fig. 3. For $\alpha=0.05$ and $\delta\phi_i=3\pi/2$, this amplitude is much higher than the maximum critical field. The assumption that $\tau_i\approx$ constant is fulfilled (see the upper inset of Fig. 5). If $\delta\phi_i=0$ the switching occurs because τ_i is decaying (cf. lower inset of Fig. 5). For extremely high values of damping a markedly different picture emerges (cf. Fig. 6). First feature observed from this figure is that after each pulse the increase in θ is roughly the same for both $\delta\phi_i=0$ and $\delta\phi_i=3\pi/2$ (consistent with the results of Fig. 1 for $\alpha=1.0$). In contrast to Fig. 5 where due to small dissipation no significant steps in ϕ have been seen, here after each magnetic pulse the system relaxes and therefore the pulses are applied every precessional period. The reversal is achieved for $\delta\phi_i=0$ for the sequence of 26 magnetic pulses. For $\delta\phi_i=3\pi/2$ it is not achievable at all. Based on the results shown in Fig. 3, one is able to explain also why the switching for $\alpha=1.0$ and $\delta\phi_i=3\pi/2$ does not occur: The field amplitude is only enough to reach the angle $\theta\approx\pi/64$. After this, relaxation begins. In contrast to that, the reversal for $\delta\phi_i=0$ and $\alpha=1.0$ is possible

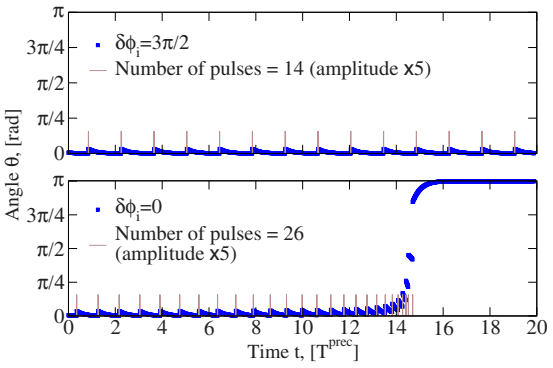

FIG. 6. (Color online) Evolution of $\theta(t)$ for $\delta\phi_i=3\pi/2$ and $\delta\phi_i=0$; $\phi_f(0)=\pi/180$, $\theta_f(0)=\pi/180$, $\phi_0=\pi/3$, $\alpha=1.0$, $b_0=0.2$, and $f(t_{0,i})=1$.

due to a dependence of $\tau_i[\theta(t_i^-)]$ which decreases the critical fields.

IV. NUMERICAL TREATMENT

In the framework of the analytical solution presented in Sec. III the questions of the angle shift $\delta\phi_i$, the critical fields $b_{0\mathrm{cr}}$, and partly the delay times between the pulses τ_i were addressed. On the other hand, the magnetization dynamics during the pulse, the effect of the form of the pulse, as well as the role of thermal fluctuations cannot be predicted analytically and have to be investigated by solving numerically for the driven Landau-Lifshitz-Gilbert equation including temperature effects. Here we utilize the approach we presented recently in Ref. 45. The analytical development of Sec. III is imperative in that it sets the range of parameters for the numerical calculations. The damping parameters are chosen as experimentally determined (Ref. 2 and references therein). Usually, for nanoparticles the typical values of damping are in the range of [0.001, 0.05]. We deliberately use the maximum damping 0.05 to speed up the relaxation process.

A. Sequence of short magnetic rectangular-shaped pulses

To inspect the validity of the short-time approximation used to derive the analytical results we consider rectangular magnetic pulses having a duration T^R, i.e.,

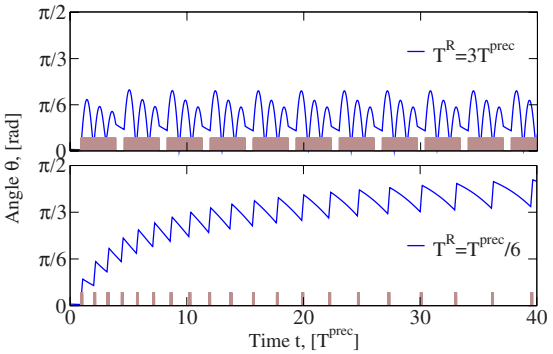

FIG. 7. (Color online) Evolution of $\theta(t)$ for different pulse durations T^R expressed in units of the precessional period. Applied pulses are shown as solid rectangles. Other parameters: $b_0^R=0.3$ and $\alpha=0.05$.

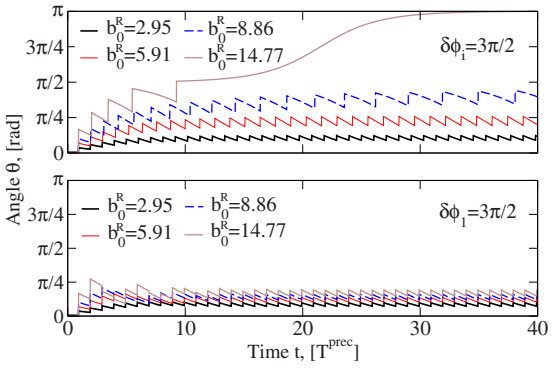

FIG. 8. (Color online) Evolution $\theta(t)$ for different strategies of pulse application: rectangular pulses are applied when $\delta\phi_i=3\pi/2$ (top); (lower panel): only the first pulse is applied when $\delta\phi_1=3\pi/2$ other pulses are delayed by a precessional period. Other parameters: $\alpha=0.05$ and $T_0=0$ K.

$$\mathbf{b}_0^R(t)=\begin{cases} b_0^R(\cos\phi_0\mathbf{e}_x+\sin\phi_0\mathbf{e}_y), & t_0-T^R<t<t_0+T^R \\ 0, & \text{elsewhere.} \end{cases} \tag{21}$$

The $\theta(t)$ evolution for different T^R is numerically calculated (Fig. 7). The control of the magnetization is achieved when the pulses are shorter than roughly $T^R<T^{\mathrm{prec}}/6$, meaning that a precise adjustment of the pulse duration is not important to achieve control. On the other hand, for pulses longer than T^{prec} the control scheme is not viable. Figures 8 and 9 illustrate two different strategies for pulse application. The first consists of applying all pulses with a certain fixed $\delta\phi$ (as in Sec. III C 6), whereas the second strategy implies the application of only the first pulse with a strictly defined $\delta\phi$ and the rest of the pulses—with a time delay of a precessional period. The second strategy allows only a freezing of the magnetization around certain θ. Figure 10 depicts the dynamics for a Co nanoparticle.[41] Due to the large damping in this case for switching, we need higher field amplitudes than for a FePt nanoparticle. For $\delta\phi_i=0$ switching is achieved for all field amplitudes starting from $b_0^R=5.91$. This procedure requires however a more frequent pulse application (cf. Fig. 11). Figure 11 additionally reveals another important feature: For certain values of b_0 one can fix both θ and ϕ in a short-

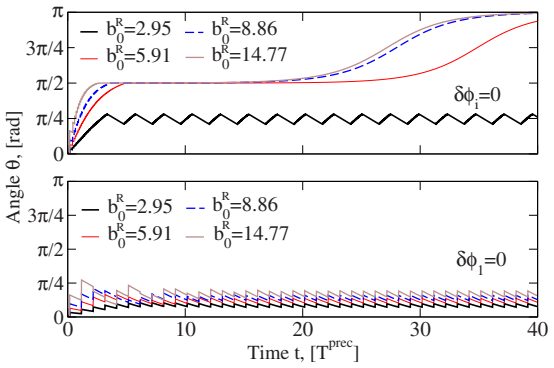

FIG. 9. (Color online) Same as in Fig. 8 with the same conditions for upper and lower panel; however, $\delta\phi_i=0$.

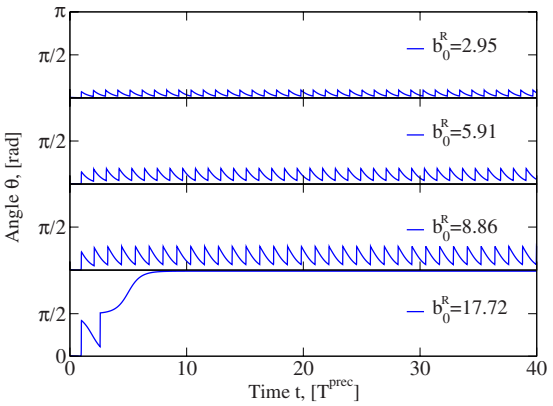

FIG. 10. (Color online) $\theta(t)$ for a Co nanoparticle for $\delta\phi_i = 3\pi/2$ and different field strengths. Other parameters: $\alpha=0.25$ and $T_0=0$ K.

time interval of approximately one precessional period. This requires a very frequent pulse application. Note that this effect, which we call "ϕ freezing" can only be performed for $\delta\phi_i=0$ [Fig. 11, Eq. (14)]. In case of $\delta\phi_i=3\pi/2$ ϕ freezing did not arise whereas a certain stabilization of θ angle was obtained for low amplitudes. The θ stabilization shown in Fig. 8 for amplitudes smaller than $b_0^R=14.77$ is similar to the effect of Larmor precession. However, the former effect can be obtained merely in a system without dissipation ($\alpha=0$). The θ stabilization occurs due to a balance in energy contributions: the energy pumped into the system by the external magnetic field and the dissipated energy due to damping. Indeed, inspecting Fig. 3 and choosing a constant amplitude of the applied pulse the balance of energies corresponds to the point where the chosen field crosses the curve. Comparing the analytical predictions with the numerical ones we find overall consistencies in results and trends. That the amplitudes calculated analytically and numerically are different is due to the different time delays, as addressed in Sec. III C 5. Furthermore, to compare b_0 and b_0^R one should contrast time integrals of the pulses (i.e., the total field action on the magnetization), i.e., $\int_{-\infty}^{\infty}\frac{b_0}{2\varepsilon}dt=b_0\int_0^1\frac{2\varepsilon}{2\varepsilon}d\tau=b_0$ and $\int_{-\infty}^{\infty}b_0^R dt=\int_{t_i^-}^{t_i^+}b_0^R dt=b_0^R(t_i^+-t_i^-)$. Hence we deduce the relation between b_0 and b_0^R,

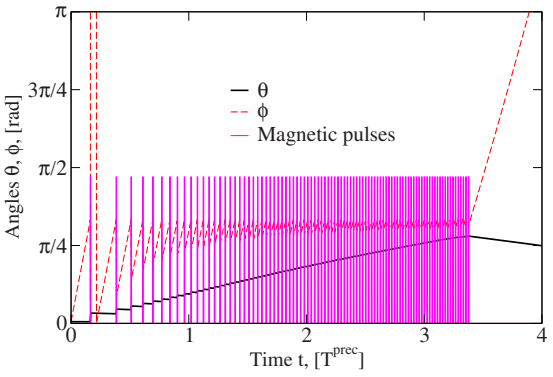

FIG. 11. (Color online) Evolution of angles θ and ϕ for $\delta\phi_i=0$ and for the parameters of the black curve shown in Fig. 9 where $b_0^R=2.95$

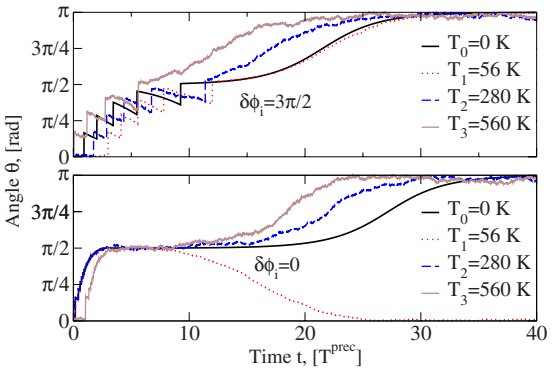

FIG. 12. (Color online) Temperature-dependent evolution of angle θ for $\delta\phi_i=3\pi/2$ (above) and $\delta\phi_i=0$ (below). Pulses are applied only when $\theta<\pi/2$. Other parameters: $\alpha=0.05$ and $b_0^R=14.77$.

$$b_0^R=\frac{b_0}{t_i^+-t_i^-}. \tag{22}$$

From this equation we can calculate the numerical critical amplitude, e.g., for $\delta\phi_i=3\pi/2$, $\alpha=0.05$, and $b_{0\mathrm{cr}}=0.05$. The numerical value should be $0.05/(6/1000)\approx 8.3$. From Fig. 8 we can deduce that starting from approximately this values switching is indeed possible; it takes, however, a longer time.

Figures 12 and 13 show the temperature-dependent time evolution of $\theta(t)$ for $\delta\phi_i=3\pi/2$ and $\delta\phi_i=0$, respectively. These figures differ merely in how long the pulses are applied: for temperature-dependent calculations it is imperative that the pulses are applied even if $\theta>\pi/2$ in order to avoid the situation shown in Fig. 12 (lower panel, $T_1=56$ K), i.e., after reaching the state $\theta=\pi/2$ the magnetization may return back to the original state due to thermal excitations. This effect is avoided by applying the pulses even if $\theta>\pi/2$ (Fig. 13).

From both figures we observe: during the pulse application even at rather high temperatures the dynamics for the short magnetic pulses remains the same as for $T=0$ K. This is explainable by the relatively high and rapid (on the scale of thermal excitations) excitation induced by the magnetic

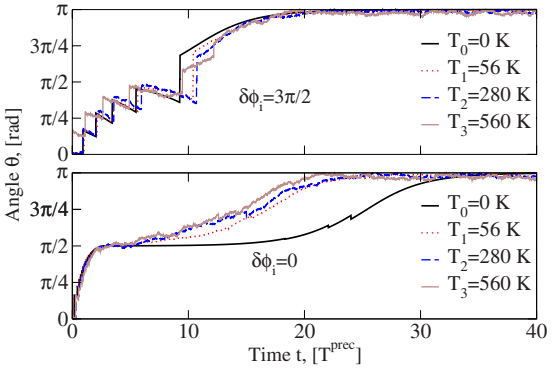

FIG. 13. (Color online) Temperature-dependent evolution of angle θ for $\delta\phi_i=3\pi/2$ (above) and $\delta\phi_i=0$ (below). Pulses are applied even when $\theta>\pi/2$. Other parameters: $\alpha=0.05$ and $b_0^R=14.77$.

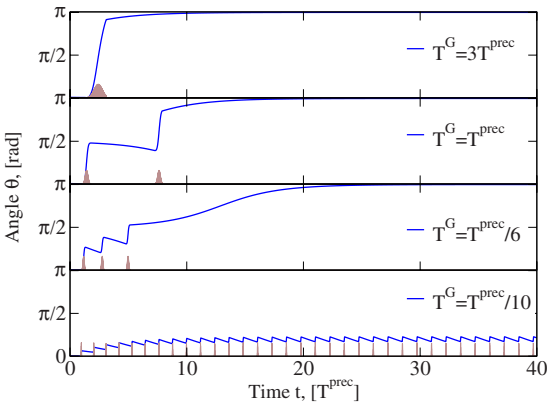

FIG. 14. (Color online) Evolution of $\theta(t)$ for different pulse durations expressed in units of the precessional period. Applied (full "bells") Gaussian pulses are shown. Other parameters: $b_0^G=1.0$ and $\alpha=0.05$.

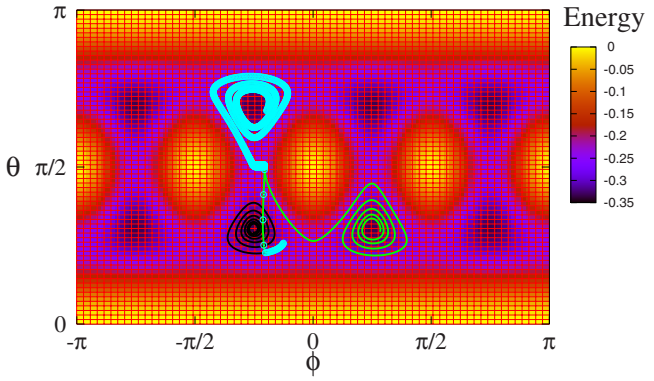

FIG. 15. (Color online) Trajectories of the magnetization on the (field-free) energy landscape corresponding to a cubic magnetic anisotropy. Results for three amplitudes of magnetic pulses are shown: $b_0^R=0$ (dark curve), $b_0^R=2.07$ (light curve), and $b_0^R=4.14$ (light points). Start conditions are: $\phi_f(0)=15\pi/8$, $\theta_f(0)=0.81$, $\phi_0=\pi/4$, $T_0=0$ K, and $\alpha=0.05$.

pulses. In the field-free regime the relaxation motion becomes strongly modified by thermal fluctuations leading thus to a rather chaotic motion of the magnetization. As shown recently by us,[34] both the effects of thermal fluctuations and the magnetization freezing, as realized within our present scheme, can be combined to induce a fast (picoseconds) thermal switching which can be utilized for fast thermal sensoring.

B. Sequence of short magnetic Gaussian-shaped pulses

We inspect here the dynamics under the influence of Gaussian-type magnetic pulses, i.e., $f(t)=2\varepsilon e^{-(t-t_0)^2/T^2}$ and Eq. (3) becomes

$$\mathbf{b}_0^G(t) = b_0^G e^{-(t-t_0)^2/T^2}(\cos\phi_0\mathbf{e}_x + \sin\phi_0\mathbf{e}_y), \qquad (23)$$

where b_0^G is the field amplitude and $T^G=6$ T is the pulse duration centered at t_0. In order to be able to compare these results with those obtained for rectangular-shaped pulses the amplitudes should be calculated from

$$b_0^R = b_0^G\sqrt{\pi}\frac{T}{t_i^+ - t_i^-}, \qquad (24)$$

which ensures that the time integral over both pulses is the same. Figure 14 depicts the dynamics for Gaussian-shaped magnetic pulses. For the same time integrals the dynamics for long pulses (Fig. 7 and 14) differs. In particular, switching might be obtained with only one Gaussian-type pulse. Short pulses for both rectangular- and Gaussian-shaped pulses have the same dynamical behavior (similar results are obtained in (Ref. 30). Thus, when aiming to study the influence of *ultra short* magnetic pulses there is no need to vary the shape of the pulses: the dynamics is the same.

C. Sequence of short magnetic pulses for a nanoparticle with a cubic anisotropy

The question of whether this scheme is valid for another anisotropy type is addressed in this subsection and depicted in Fig. 15. For a cubic anisotropy [Eq. (9)] switching can be defined either as a reversal to the closest stable state or as a reversal to the antiparallel state. We demonstrate within the scheme proposed that switching to the closest state is possible and also into the negative semisphere by increasing the field amplitudes. The magnetic pulses are only applied for the fixed angular shift $\delta\phi_i=3\pi/2$ and when $\theta<\pi/2$. The light curves for nonzero amplitudes show a switching from one stable orientation to another one. Note that when the pulses are applied the magnetization experiences a quasiballistic switching.

V. CONCLUSIONS AND DISCUSSION

In this paper the dynamical behavior of the nanoparticle's magnetization was studied on the basis of the Landau-Lifshitz-Gilbert equation of motion both analytically and numerically. A scheme was proposed specifying the conditions under which a controlled magnetization reversal is achieved. The analytical solution reveals the general dependencies. Expressions are provided for the value of the magnetization change upon the pulse application and for the critical (minimal) field $b_{0\mathrm{cr}}$ needed for switching. The dependencies of $b_{0\mathrm{cr}}$ on the damping parameter and the total field amplitude as well as on the ratio of the applied field strengths are also given. The scheme is universal in that it does not depend on the type of magnetic anisotropy as long as the pulse is shorter that the precessional period. The field-free magnetization dynamics intervening the pulses is, however, anisotropy dependent. The finite-temperature numerical procedure endorsed the robustness of the analytical predictions to a variation in the duration of the pulses and to thermal fluctuations. The critical switching fields expressed in units of the maximum anisotropy field depend on the applied field-strength ratio contained in and on the damping parameter as well as on the field-free time between pulses. Analytical expressions for the critical field amplitudes are basically confirmed numerically. For high field amplitudes less pulses are needed for switching. Another feature of the present control scheme is the magnetization freezing, i.e., for certain field-

amplitude strengths, which are given in explicit form; the magnetization can be steered to a predefined angular position and roughly stabilized there. As for temperature effects, they turned out to be of a minor importance during the pulse application. However, thermal fluctuations influence strongly the relaxation process in between the pulses. For pulses with a duration shorter than the precessional period we confirm the independence of the qualitative behavior of the magnetization dynamics on the pulse shapes.

Experimentally the proposed control scheme may be realized in an experimental setup similar to that reported in Ref. 28. The pulse strength achieved in Ref. 28 can be as high as some Tesla, the pulse duration however is some picoseconds,[27] which restricts the applicability of our scheme to certain materials with a longer precessional period. Another promising possibility is the use light pulses (which can be as short as attoseconds) to generate the required magnetic fields.[50–52]

ACKNOWLEDGMENTS

This work is supported by the International Max Planck Research School for Science and Technology of Nanostructures.

[1] *Spindynamics in Confined Magnetic Structures III*, edited by B. Hillebrands and K. Ounadjela (Springer, Berlin, 2002); *Spin Dynamics in Confined Magnetic Structures II*, edited by B. Hillebrands and K. Ounadjela (Springer, Berlin, 2002), and references therein.
[2] *Spin Dynamics in Confined Magnetic Structures I*, edited by B. Hillebrands and K. Ounadjela (Springer, Berlin, 2002).
[3] *Magnetic Nanostructures*, Springer Series in Materials Science Vol. 94 edited by B. Aktas, L. Tagirov, and F. Mikailov (Springer, New York, 2007).
[4] M. Vomir, L. H. F. Andrade, L. Guidoni, E. Beaurepaire, and J.-Y. Bigot, Phys. Rev. Lett. **94**, 237601 (2005).
[5] A. V. Kimel, A. Kirilyuk, P. A. Usachev, R. V. Pisarev, A. M. Balbashov, and Th. Rasing, Nature (London) **435**, 655 (2005).
[6] C. A. Perroni and A. Liebsch, Phys. Rev. B **74**, 134430 (2006).
[7] E. C. Stoner and E. P. Wohlfarth, Philos. Trans. R. Soc. London, Ser. A **240**, 599 (1948).
[8] L. He, W. D. Doyle, and H. Fujijava, IEEE Trans. Magn. **30**, 4086 (1994).
[9] G. Bertotti, C. Serpico, and I. D. Mayergoyz, Phys. Rev. Lett. **86**, 724 (2001).
[10] C. Thirion, W. Wernsdorfer, and D. Mailly, Nature Mater. **2**, 524 (2003).
[11] Y. Acremann, C. H. Back, M. Buess, O. Portmann, V. Vaterlaus, D. Pescia, and H. Melchior, Science **290**, 492 (2000).
[12] G. Woltersdorf and C. H. Back, Phys. Rev. Lett. **99**, 227207 (2007).
[13] Y. Nozaki and K. Matsuyama, J. Appl. Phys. **100**, 053911 (2006).
[14] H. K. Lee and Z. Yuan, J. Appl. Phys. **101**, 033903 (2007).
[15] Z. Z. Sun and X. R. Wang, Phys. Rev. Lett. **97**, 077205 (2006).
[16] S. I. Denisov, T. V. Lyutyy, P. Hänggi, and K. N. Trohidou, Phys. Rev. B **74**, 104406 (2006).
[17] Y. Nozaki, M. Ohta, S. Taharazako, K. Tateishi, S. Yoshimura, and K. Matsuyama, Appl. Phys. Lett. **91**, 082510 (2007).
[18] J. Slonczewski, J. Magn. Magn. Mater. **159**, L1 (1996).
[19] L. Berger, Phys. Rev. B **54**, 9353 (1996).
[20] M. Tsoi, A. G. M. Jansen, J. Bass, W. C. Chiang, M. Seck, V. Tsoi, and P. Wyder, Phys. Rev. Lett. **80**, 4281 (1998).
[21] E. B. Myers, D. C. Ralph, J. A. Katine, R. N. Louie, and R. A. Buhrman, Science **285**, 867 (1999).
[22] Z. Li and S. Zhang, Phys. Rev. B **68**, 024404 (2003).
[23] S. Mangin, D. Ravelsona, J. A. Katine, M. J. Carey, B. D. Terris, and E. E. Fullerton, Nature Mater. **5**, 210 (2006).
[24] X. R. Wang and Z. Z. Sun, Phys. Rev. Lett. **98**, 077201 (2007).
[25] Y. Tserkovnyak, A. Brataas, and G. E. W. Bauer, J. Magn. Magn. Mater. **320**, 1282 (2008).
[26] L. He and W. D. Doyle, J. Appl. Phys. **79**, 6489 (1996).
[27] C. H. Back, D. Weller, J. Heidmann, D. Mauri, D. Guarisco, E. L. Garwin, and H. C. Siegmann, Phys. Rev. Lett. **81**, 3251 (1998).
[28] C. H. Back and H. C. Siegmann, J. Magn. Magn. Mater. **200**, 774 (1999).
[29] T. Gerrits, H. A. M. van den Berg, J. Hohlfeld, L. Bär, and Th. Rasing, Nature (London) **418**, 509 (2002).
[30] M. Bauer, J. Fassbender, B. Hillebrands, and R. L. Stamps, Phys. Rev. B **61**, 3410 (2000).
[31] H. Xi, K. Z. Gao, and S. Xue, J. Appl. Phys. **103**, 07F502 (2008); P. P. Horley, V. R. Vieira, P. M. Gorley, V. K. Dugaev, J. Berakdar, and J. Barnas, Phys. Rev. B **78**, 054417 (2008).
[32] H. W. Schumacher, C. Chappert, R. C. Sousa, P. P. Freitas, and J. Miltat, Phys. Rev. Lett. **90**, 017204 (2003).
[33] C. H. Back, R. Allenspach, W. Weber, S. S. P. Parkin, D. Weller, E. L. Garwin, and H. C. Siegmann, Science **285**, 864 (1999).
[34] A. Sukhov and J. Berakdar, Phys. Rev. Lett. **102**, 057204 (2009).
[35] R. Kosloff, A. D. Hammerich, and D. J. Tannor, Phys. Rev. Lett. **69**, 2172 (1992).
[36] S. Gräfe, C. Meier, and V. Engel, J. Chem. Phys. **122**, 184103 (2005).
[37] P. Marquetand and V. Engel, J. Phys. B **41**, 074026 (2008).
[38] M. Shapiro and P. Brumer, *Principles of Quantum Control of Molecular Processes* (Wiley, New York, 2003).
[39] D. J. Tannor, *Introduction to Quantum Mechanics: A Time-dependent Perspective* (University Science Books, New York, 2007), and references therein.
[40] C. Antoniak, J. Lindner, M. Spasova, D. Sudfeld, M. Acet, M. Farle, K. Fauth, U. Wiedwald, H. G. Boyen, P. Ziemann, F. Wilhelm, A. Rogalev, and S. Sun, Phys. Rev. Lett. **97**, 117201 (2006).
[41] W. T. Coffey, D. S. F. Crothers, J. L. Dormann, Yu. P. Kalmykov, E. C. Kennedy, and W. Wernsdorfer, Phys. Rev. Lett. **80**, 5655 (1998).
[42] C. Antoniak, J. Lindner, and M. Farle, Europhys. Lett. **70**, 250 (2005).
[43] L. Landau and E. Lifshitz, Phys. Z. Sowjetunion **8**, 153 (1935).

[44] T. L. Gilbert, Phys. Rev. **100**, 1243 (1955) [Abstract only; full report, Armor Research Foundation Project No. A059, Supplementary Report, May 1, 1956] (unpublished); IEEE Trans. Magn. **40**, 3443 (2004).
[45] A. Sukhov and J. Berakdar, J. Phys.: Condens. Mater **20**, 125226 (2008).
[46] Z. Z. Sun and X. R. Wang, Phys. Rev. B **71**, 174430 (2005).
[47] J. L. García-Palacios and F. J. Lázaro, Phys. Rev. B **58**, 14937 (1998).
[48] *Physics of Ferromagnetism S. Chikazumi* (Oxford University Press, New York, 1997), p. 250.
[49] I. Mayergoyz, M. Dimian, G. Bertotti, and C. Serpico, J. Appl. Phys. **97**, 10A703 (2005).
[50] A. S. Moskalenko, A. Matos-Abiague, and J. Berakdar, Phys. Rev. B **74**, 161303(R) (2006).
[51] T. Lehner, Europhys. Lett. **50**, 480 (2000).
[52] J. C. Mallinson, IEEE Trans. Magn. **36**, 1976 (2000).